PHYSICAL REVIEW B VOLUME 20, NUMBER 12 15 DECEMBER 1979

Hard-core pseudopotentials and structural maps of solids

W. Andreoni* and A. Baldereschi
Laboratoire de Physique Appliquée, EPF, Lausanne, Switzerland

E. Biémont
Institut d'Astrophysique, Université de Liège, Cointe-Ougrée, Belgium

J. C. Phillips
Bell Laboratories, Murray Hill, New Jersey 07974
(Received 2 August 1979)

A simple nonlocal hard-core model pseudopotential which reproduces Hartree-Fock energies and wave functions is proposed for the hydrogenic ions of the Li, Na, K, and Cu isoelectronic series. These l-dependent model pseudopotentials are used to obtain improved orbital radii and new structural coordinates for $A^N B^{8-N}$ octet compounds. A successful classification of the crystal structures is obtained for this family of materials. The relationship between our orbital radii and those previously suggested by Simons, Bloch, St. John, Chelikowsky and Phillips, and Zunger and Cohen is discussed.

I. INTRODUCTION

For many years both experimentalists and theorists have used pseudopotentials to describe the electronic properties of solids. In early work[1,2] the form of the pseudopotential $V_p(r)$ was chosen to give rapid damping of the Fourier transform $\tilde{V}_p(q)$ for large $q \gtrsim 2k_p$. This choice emphasized the nearly free-electron nature of the Bloch energy bands $E_n(k)$, which is a characteristic property of metals and semiconductors formed from nontransition elements. Moreover, this choice of soft-core pseudopotentials was suggested by the similarity of the approach to the Herring orthogonalized-plane-wave method for solving rigorously the wave equation in solids.[3] In fact, in a famous paper describing the cancellation of valence and kinetic energies in the core region, Cohen and Heine argued[4] that suitably chosen soft-core pseudopotentials could give better Bloch energy bands, in a truncated basis set of 100 plane waves or fewer that could the rigorous, orthogonalized-plane-wave (OPW) parent. This argument won support as much for its suitability to the computational state of the art at that time as for its persuasive formal analogies.

The primary interest for the last 50 years in quantum studies of solids has been one-electron levels. The structural properties of solids, which involve the total electronic energy, have largely been treated empirically, e.g., by Mooser and Pearson (MP) for intermetallic compounds[5] or Phillips and Van Vechten (PVV) for more than 80 $A^N B^{8-N}$ binary semiconductors and insulators[6] with eight s-p valence electrons per atom pair. However, Simons, Bloch, and St. John have recently discovered[7-9] that it is possible to use pseudopotential core radii, derived only from hydrogenic-ion-term values, to construct structural maps for elemental metals and $A^N B^{8-N}$ compounds. Their work has been extended[10,11] to more than 50 metallic compounds composed of nontransition elements; the results are, in general, significantly more successful than the empirical structural maps, which is quite surprising considering the atomistic origin of the pseudopotential parameters.

There are two characteristics of the Simons-Bloch (SB) pseudopotentials, as utilized to form structural maps, which differentiate them from the pseudopotentials used in energy-band studies. The latter have soft cores, and $V_p(r)$ is weak for $r \to 0$, whereas the SB pseudopotentials have hard cores, with $V_p(r) \to \text{const}/r^2$ as $r \to 0$. In retrospect, this should not be surprising, for even metallic compounds formed from nontransition elements exhibit complex crystal structures.[10,11] With soft-core pseudopotentials one can utilize perturbation methods[12,13] which predict, in general, a marked tendency toward simple structures (close-packed, body-centered-cubic, etc.). Thus hard-core effects must be substantial if we are to be able to explain the common occurrence of complex crystal structures even with nontransition elements.

The second distinguishing characteristic of SB pseudopotentials is that they are explicitly l dependent. In studies of one-electron energy

levels near $E=E_F$ (the Fermi energy) in metals or in semiconductors, it has generally been found to be sufficient to use an effective local pseudopotential form factor $\tilde{V}_p(q)$, describing the scattering between states k and $k+q$ such that $|k| = |k+q| = k_F$ (on-Fermi-surface scattering), which involves averaging over s and p (and, to a lesser extent for nontransition elements, d) pseudopotentials. (Exceptions where nonlocal corrections are important arise when the experimental data warrant 1% accuracy in one-electron energy differences, e.g., in Ge and GaAs.[14]) Of course, complex coordination configurations imply significant covalent bonding, even in metallic compounds, and the degree of hybridization among s, p, and (for transition metals) d states determines the nature of covalent bonds. Thus we are not surprised to learn that l-dependent coordinates are needed to derive structural maps. What *is* surprising is that the structural coordinates derived from SB pseudopotentials combine l-dependent radii in a *linear* way, so that the algebraic basis (and physical interpretation) of the structural maps becomes almost too obvious.

Certainly the very difficult problem of differentiating complex crystal structures should not be solved by a linear algebra based on free-ion-term values, but the empirical success of the structure maps is far too great to be accidental. A serious weakness in the SB pseudopotentials was evident to Baldereschi and Meloni, who noted[15] that, because the const/r^2 term extended to large r as well as small r, the SB pseudopotential is too repulsive at large r, which has the effect of compressing the wave functions. For the SB procedure to have physical meaning, one should demand that *both* the energy and the maximum of the valence-electron pseudowave function match the energy and outer maximum of the Hartree-Fock atomic wave function; in this way the model includes enough information to make meaningful orbital (l-dependent) structural predictions.

As is often the case with very successful, oversimplified theories, when these improvements were made in SB pseudopotentials, large changes in the radial orbital parameters were found.[16] Although spectacular two-parameter fits to the HF atomic wave functions were achieved, not only at the outer maximum but practically down to the outer node as well, the changes in the s radii were found to be much greater than the changes for the p radii. These results were obtained only for elements from the first period, but clearly they raised great problems for devising structural maps from coordinates derived from orbital radii. In this paper we have therefore derived refined (or renormalized) orbital radii for elements belonging to the later periods as well, in an effort to resolve these problems.

II. ATOMIC MODEL PSEUDOPOTENTIALS AND ORBITAL RADII

Nonrelativistic Hartree-Fock (HF) wave functions $\Psi_{nl}^{HF}(r)$ have been calculated for $l=0, 1, 2$ and for the hydrogenic ions of the Li, Na, K, and Cu isoelectronic series using the method developed by Froese-Fischer.[17] Rb and Cs have also been studied in order to complete the group of alkali-metal atoms. The calculated HF valence energies[18] E_{nl}^{HF} differ from experimental energies[19] E_{nl} by a few percent, apart from the cases of Cu, Rb, and Cs, where differences $\Delta E_{nl} = E_{nl}^{HF} - E_{nl}$ are for some l values larger than 10% (for Cu, $\Delta E_{40} \cong 0.16 E_{40}$, $\Delta E_{41} \cong 0.14 E_{41}$, for Rb, $\Delta E_{50} \cong 0.10 E_{50}$, for Cs, $\Delta E_{60} \cong 0.14 E_{60}$, $\Delta E_{62} \cong 0.12 E_{62}$). These discrepancies are due to electron-electron correlations and, to a minor extent, to relativistic corrections. According to relativistic Hartree-Fock calculations by Desclaux,[20] relativistic corrections amount to 2%, 3%, and 4% in Rb, Cu, and Cs, respectively. Electron-electron correlations mostly affect the HF valence energies through core-charge polarization,[21] i.e., the distortion of the outer core shells due to the presence of the valence electron, which, in turn, feels an additional self-induced polarization potential. Core polarization becomes more relevant as the atomic number increases and is dominated by dipole terms which are not taken into account in any self-consistent field theory where the valence electron is subject to a spherically symmetric potential. This effect has so far been quantitatively studied in a few calculations only[22-24] and has been shown to explain the order of magnitude of the deviations between experimental and HF energies.

We have then constructed a simple, nonlocal, hard-core model pseudopotential[16] which is able to fit HF energies and valence HF wave functions from infinity down to the outer node. Our pseudopotential is l dependent and is written as

$$V_l(r) = -\frac{2Z}{r} + W_l(r), \tag{1a}$$

where Z is the core charge and $W_l(r)$ is a two-parameter short-range potential

$$W_l(r) = A_l \frac{e^{-\gamma_l r}}{r^2}, \tag{1b}$$

which corresponds to Simons's one-parameter model (B_l/r^2) times a damping factor which describes the confinement to the core region of the

short-range orthogonality, electrostatic, and exchange interactions of the valence electron with core electrons. If the core contains electrons with the same angular momentum l as the valence electron, $W_l(r)$ is dominated by orthogonality repulsions ($A_l > 0$) and strongly confined within the ionic core. If the valence electron is already orthogonal to all core electrons because of its angular momentum (as it is the case for valence p or d states of Li-like ions), $W_l(r)$ is attractive ($A_l < 0$), since it contains electrostatic and exchange terms only.

For each ion and each l, the two parameters A_l and γ_l are obtained by fitting, for the lowest valence state of the given l, the HF energy and the position of the outer maximum of the corresponding HF function. When we apply Eq. (1) to Li-like ions, our model for $W_l(r)$ is very accurate in reproducing HF wave functions outside the outermost node.[16] For the $2s$ states the repulsive (orthogonality) term in the valence-core interactions dominates, and the exponent γ_0 in the damping function turns out to be simply related to the atomic number Z_N [$\gamma_0 = 2Z_N = 2(Z+2)$] and to the inverse of the exponential decay length of the $1s$ core wave function which is also proportional to Z_N. The valence $2p$ states are almost hydrogenic, and the weak core attraction can be well described by the short-range potential Eq. (1b). The parameter γ_1 is smaller than γ_0 because the exchange-attractive interactions are more delocalized in real space than the orthogonality effects. On passing to successive rows in the Periodic Table (Na-like, K-like, and Cu-like ions), we obtained $\gamma_0 = \gamma_1 = 2(Z+2)$ as the best value to fit the position of the maximum of s and p valence wave functions.

Valence d states behave differently for different rows of the Periodic Table, and they require, therefore, special treatment. In Cu-like ions, the valence d states are orthogonal to $3d$ core electrons, and our model gives very accurate results with $\gamma_2 = \gamma_0 = \gamma_1$. In Li-like ions, $3d$ states are mostly hydrogenic, and very good wave functions can be obtained with a model potential having the same exponential decay as for p states ($\gamma_2 = \gamma_1$). Our model Eq. (1b) starts to lose accuracy for Na-like ions and definitely fails ($A_2 < -6$) for the core-penetrating d orbits of K-like ions and for Rb and Cs. In order to solve this problem, in all these cases we have replaced (1b) with

$$\tilde{W}_2(r) = \tilde{A}_2 e^{-\tilde{\gamma}_2 r} . \tag{1c}$$

Our model pseudopotential is very accurate for Li-like ions and accurate still for Na-like ions, but the accuracy decreases for higher periods in the Periodic Table since valence and core orbits become closer and closer, and the valence electrons feel more the short-range attractive interactions with the core. This fact can be easily seen by comparing the position of the outer maximum of the actual wave function R_l^{HF} and of the pseudowave function R_l^{PS} (Table I) for isovalent atoms. Within a given period of the Periodic Table, our fit to HF wave functions improves with higher valence. Once again this is due to the short-range valence-core attractive interactions whose strength increases with Z more slowly than that of the long-range Coulomb interaction.

All our results for the model potential are collected in Table II, in which we give the values of the parameters A_l and γ_l in (1b) and $\tilde{A}_2$ and $\tilde{\gamma}_2$ in (1c). In Fig. 1 we report our s, p, d model pseudopotentials for the tetravalent ions, and in

TABLE I. Comparison of the positions of the outer maxima of the HF wave functions (upper line) and of our pseudowave functions (lower line and in parentheses) for several elements and for $l = 0, 1, 2$. All data are in atomic units.

Li	C^{3+}	Ne^{7+}
2.026, 1.688, 5.994	0.787, 0.438, 1.496	0.439, 0.231, 0.748
(2.021, 1.687, 5.998)	(0.783, 0.438, 1.497)	(0.436, 0.231, 0.748)
Na	Si^{3+}	Ar^{7+}
2.311, 3.159, 5.948	1.319, 1.405, 1.282	0.885, 0.879, 0.617
(2.283, 3.156, 5.949)	(1.312, 1.400, 1.282)	(0.883, 0.876, 0.614)
K	Ti^{3+}	Fe^{7+}
3.220, 4.128, 0.707	2.013, 2.234, 0.495	1.435, 1.507, 0.360
(3.153, 4.274, 0.707)	(1.991, 2.224, 0.495)	(1.432, 1.499, 0.360)
Cu	Ge^{3+}	Kr^{7+}
1.812, 2.447, 6.216	1.378, 1.536, 2.085	1.078, 1.140, 1.295
(1.440, 2.118, 6.216)	(1.335, 1.501, 2.080)	(1.065, 1.129, 1.288)

TABLE II. Values of the parameters of our nonlocal hard-core model pseudopotentials: (A_l, γ_l) in Eq. (1b) and $(\tilde{A}_2, \tilde{\gamma}_2)$ in Eq. (1c). All data are in atomic units.

			Li-like Ions			
	γ_0	A_0	γ_1	A_1	γ_2	A_2
Li	6	2233.85	2.02	−1.074	2.02	−0.600
Be^{+}	8	1518.15	2.45	−1.026	2.45	−0.400
B^{2+}	10	1241.36	2.87	−0.716	2.87	−0.280
C^{3+}	12	1096.70	3.30	−0.547	3.30	−0.200
N^{4+}	14	1008.26	3.73	−0.441	3.73	−0.158
O^{5+}	16	948.70	4.15	−0.368	4.15	−0.130
F^{6+}	18	906.00	4.58	−0.316	4.58	−0.110
Ne^{7+}	20	873.85	5.01	−0.278	5.01	−0.095
			Na-like Ions			
	γ_0	A_0	γ_1	A_1	$\tilde{\gamma}_2$	$\tilde{A}_2$
Na	6	6 820	6	21 280	2.805	−20.150
Mg^{+}	8	26 430	8	44 990	3.520	−35.980
Al^{2+}	10	71 323	10	81 560	4.235	−53.200
Si^{3+}	12	154 250	12	131 700	4.950	−71.545
P^{4+}	14	287 000	14	195 100	5.665	−90.651
S^{5+}	16	479 050	16	270 900	6.380	−110.350
Cl^{6+}	18	737 000	18	357 730	7.095	−130.496
Ar^{7+}	20	1 064 600	20	454 120	7.810	−151.040
			K-like Ions			
	γ_0	A_0	γ_1	A_1	$\tilde{\gamma}_2$	$\tilde{A}_2$
K	6	2.7470×10^{5}	6	4.2700×10^{6}	2.58	−82.0645
Ca^{+}	8	2.9627×10^{6}	8	2.4562×10^{7}	3.12	−100.3762
Sc^{2+}	10	1.9030×10^{7}	10	1.0470×10^{8}	3.56	−119.7255
Ti^{3+}	12	8.7580×10^{7}	12	3.5400×10^{8}	3.97	−136.9645
V^{4+}	14	3.1710×10^{8}	14	1.0001×10^{9}	4.37	−153.7951
Cr^{5+}	16	9.5760×10^{8}	16	2.4460×10^{9}	4.77	−170.9730
Mn^{6+}	18	2.5113×10^{9}	18	5.3690×10^{9}	5.15	−186.6820
Fe^{7+}	20	5.8518×10^{9}	20	1.0735×10^{10}	5.53	−202.5975
Co^{8+}	22	1.2520×10^{10}	22	1.9822×10^{10}	5.90	−217.7861
Ni^{9+}	24	2.4591×10^{10}	24	3.4466×10^{10}	6.27	−233.1084
			Cu-like Ions			
	γ_0	A_0	γ_1	A_1	γ_2	A_2
Cu	6	1.8361×10^{2}	6	2.3550×10	6	4.4800×10^{5}
Zn^{+}	8	4.5480×10^{3}	8	7.3600×10^{3}	8	9.6800×10^{5}
Ga^{2+}	10	3.6950×10^{4}	10	6.8890×10^{4}	10	2.2037×10^{6}
Ge^{3+}	12	1.9240×10^{5}	12	3.5340×10^{5}	12	4.7308×10^{6}
As^{4+}	14	7.6990×10^{5}	14	1.3395×10^{6}	14	9.4580×10^{6}
Se^{5+}	16	2.5631×10^{6}	16	4.1700×10^{6}	16	1.7699×10^{7}
Br^{6+}	18	7.4195×10^{6}	18	1.1243×10^{7}	18	3.1249×10^{7}
Kr^{7+}	20	1.9210×10^{7}	20	2.7103×10^{7}	20	5.2417×10^{7}
			Heavier alkalis			
	γ_0	A_0	γ_1	A_1	$\tilde{\gamma}_2$	$\tilde{A}_2$
Rb	6	1.096×10^{6}	6	4.28×10^{7}	1.734	−24.93
Cs	6	1.309×10^{7}	6	7.56×10^{8}	1.244	−11.39

Fig. 2 we compare pseudowave functions and HF functions for the lowest valence s state of these ions. With our model potential we reproduce both energies and wave functions with high accuracy, and, therefore, our approach represents a considerable advance over Simons's model, whose pseudowave functions compare badly with the actual ones even for light elements.[16] Furthermore, our model retains the chemical regularity of Simons's model. In the latter case the reg-

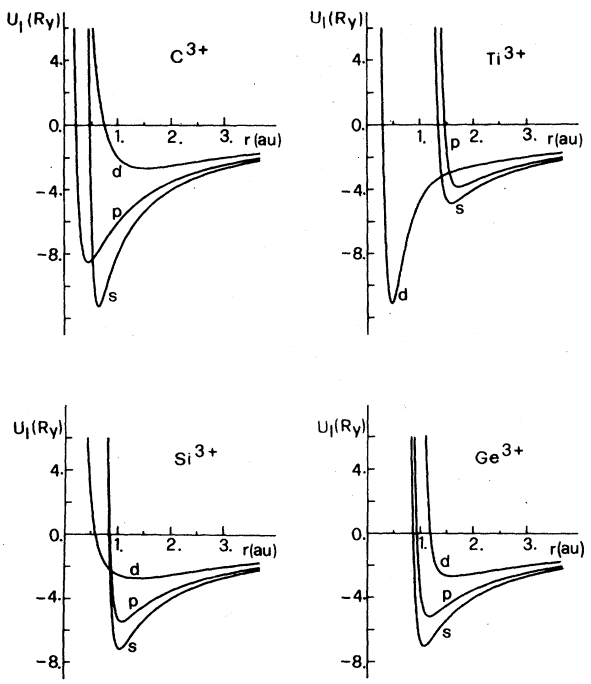

FIG. 1. s, p, d model pseudopotentials $U_l(r) = V_l(r) + l(l+1)/r^2$ for C^{3+}, Si^{3+}, Ti^{3+}, and Ge^{3+} [$V_l(r)$ is defined in Eq. (1)].

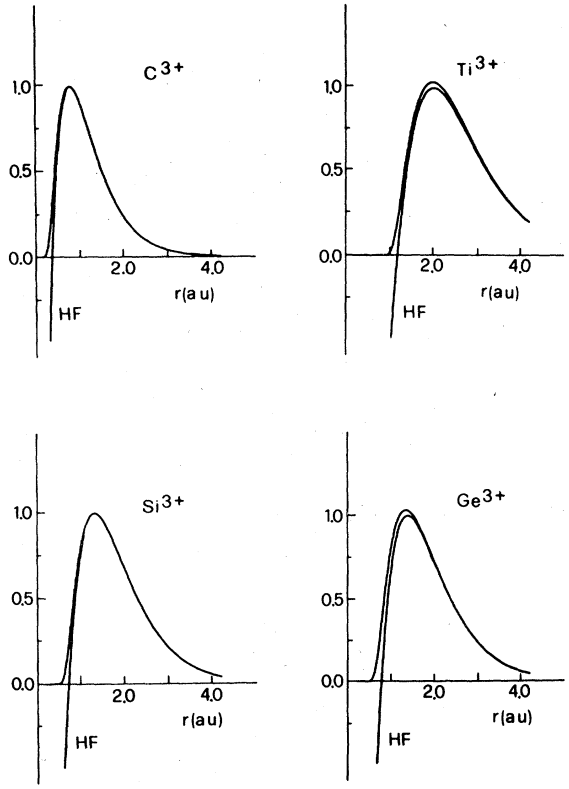

FIG. 2. Comparison of the lowest s wave function of the hard-core pseudopotential to the HF wave function of the outer s electron for C^{3+}, Si^{3+}, Ti^{3+}, and Ge^{3+}. For each ion, the normalized wave functions have been scaled so that at its outer maximum the HF function has the value 1 a.u. The scaling factors are 0.98 (C^{3+}), 1.79 (Si^{3+}), 2.99 (Ti^{3+}), and 1.85 (Ge^{3+}).

ularity originates from the fact that the model contains only one parameter, the quantum defect l', and this parameter is adjusted to the energy eigenvalues which exhibit high regularity in the Periodic Table. In our case the exponent γ_l does not depend on l when $W_l(r)$ represents the same type of interactions, and it does not change appreciably along the columns, since it mostly depends on the core charge Z and not on the nuclear charge Z_N.

Having defined our model pseudopotential, we can now calculate the orbital radii, i.e., the classical turning points for zero energy,[25] to be used for structural maps in the next section. Our pseudopotential being more physical than the SB model, we can reasonably expect that the corresponding orbital radii S_l^{PS} will be more meaningful. The difficulties that we encountered for a few atoms in fitting the position of the maximum of the radial wave function are the main source of inaccuracy of our pseudopotentials and orbital radii S_l^{PS}. To achieve better accuracy we have scaled our S_l^{PS} values according to $S_l = (R_l^{HF}/R_l^{PS})S_l^{PS}$, which reflects the fact that at constant valence energy, a larger value of R_l is obtained with a larger orbital radius. We estimate that the uncertainty in our scaled orbital radii S_l is less than 10%, even for those atoms such as Zn where the valence wave functions are not too well reproduced by our model pseudopotential. In Table III we compare our scaled S_l values to those of SB which are obtained by fitting to HF energies only. Quite relevant differences exist between the two sets of radii. For s radii, the ratio (S_0/S_0^{SB}) is almost constant and ranges from 2.5 to 2.8, while p-radii ratios behave quite differently for different rows. For Li-like ions with hydrogenic-like p states, $(S_1/S_1^{SB}) \sim 1$, while for the other rows $S_1 > S_1^{SB}$ by a factor which ranges from 1.2 to 2.5.

In an attempt to include Cu, Rb, and Cs compounds in our structural plots, we have added in Table II the pseudopotential parameters for these atoms. As discussed above, the HF approach is less accurate for these atoms, due to larger core-polarization effects. The core-polarization potential[22-24] is attractive and quite long-ranged and therefore significantly increases the valence

TABLE III. Values of the classical turning points of our model pseudopotentials (S_l) and of the SB model (S_l^{SB}) corresponding to HF energies. All data are in atomic units.

	S_0	S_0^{SB}	S_1	S_1^{SB}	S_2	S_2^{SB}
Li	1.150	0.475	0.841	0.957	2.999	3.000
Be^{+}	0.776	0.317	0.404	0.472	1.497	1.499
B^{2+}	0.589	0.238	0.280	0.315	0.997	0.999
C^{3+}	0.475	0.193	0.217	0.238	0.748	0.750
N^{4+}	0.397	0.162	0.176	0.191	0.598	0.600
O^{5+}	0.342	0.139	0.150	0.160	0.499	0.500
F^{6+}	0.300	0.123	0.130	0.138	0.427	0.428
Ne^{7+}	0.266	0.109	0.115	0.121	0.374	0.375
Na	1.327	0.544	1.626	1.215	2.979	2.993
Mg^{+}	1.096	0.443	1.212	0.732	1.362	1.478
Al^{2+}	0.951	0.379	0.997	0.551	0.812	0.970
Si^{3+}	0.841	0.333	0.854	0.449	0.579	0.718
P^{4+}	0.756	0.298	0.751	0.383	0.458	0.570
S^{5+}	0.689	0.270	0.672	0.335	0.383	0.472
Cl^{6+}	0.632	0.247	0.609	0.299	0.331	0.403
Ar^{7+}	0.583	0.227	0.557	0.270	0.294	0.352
K	1.908	0.775	2.295	1.472	0.441	2.278
Ca^{+}	1.651	0.653	1.901	0.980	0.384	0.809
Sc^{2+}	1.478	0.574	1.647	0.780	0.330	0.457
Ti^{3+}	1.342	0.516	1.458	0.662	0.292	0.348
V^{4+}	1.231	0.470	1.315	0.581	0.263	0.291
Cr^{5+}	1.138	0.432	1.198	0.520	0.239	0.255
Mn^{6+}	1.059	0.400	1.107	0.472	0.220	0.229
Fe^{7+}	0.989	0.373	1.027	0.433	0.204	0.209
Co^{8+}	0.935	0.350	0.958	0.401	0.191	0.193
Ni^{9+}	0.882	0.330	0.900	0.374	0.179	0.179
Zn^{+}	0.975	0.365	1.081	0.667	1.734	1.574
Ga^{2+}	0.929	0.356	1.012	0.545	1.382	1.096
Ge^{3+}	0.882	0.340	0.946	0.477	1.181	0.856
As^{4+}	0.838	0.322	0.887	0.426	1.045	0.710
Se^{5+}	0.797	0.306	0.835	0.389	0.944	0.611
Br^{6+}	0.759	0.290	0.788	0.360	0.864	0.538
Kr^{7+}	0.726	0.276	0.748	0.335	0.798	0.483
Rb	2.139	0.861	2.728	1.753	0.651	2.713
Cs	2.537	1.016	3.188	1.595	1.176	2.329

binding energy and reduces each orbital radius S_l to a smaller value S_l'. Generally, however, this potential is smooth compared to the orthogonality repulsion, and so it has little effect on the orbital radius ($\Delta S_l \equiv S_l - S_l'$). We have numerically verified that this is the case for Cs, where accurate l-dependent polarization model potentials are available[23] for $l=0,1$. We find that $\Delta S_0 = 0.006 S_0$ and $\Delta S_1 = 0.004 S_1$. To our knowledge, no core-polarization model potential has yet been proposed for Rb, but we expect that the effect of polarization on the Rb orbital radii will be similar to that quoted above for Cs. The case of Cu is different from those of Rb and Cs. Here, core-polarization effects are rather strong and, at the same time, the orthogonality repulsion is not as sharp and strong as in the other atoms (see the parameters in Table II). Consequently, when the polarization potential for Cu is added[24] to our model, the changes ΔS_l turn out to be $\Delta S_0 = 0.05 S_0$, $\Delta S_1 = 0.27 S_1$, and $\Delta S_2 = 0.09 S_2$. We notice that among the ions of the Cu isoelectronic sequence, only for Cu has the polarization of the core such large effects on orbital radii. The changes ΔS_l due to core polarization[24] are in fact less than 2% in Zn, less than 1% in Ga, and of the order of a few percent for all the other atoms. We conclude therefore that, with the exception of Cu, the values of ΔS_l are all within the overall computational accuracy of our orbital radii. Therefore, we will include Cs and Rb compounds in our structural plots, without changing the values of their orbital radii, but we will not consider Cu compounds, since we believe that accurate orbital radii for Cu require a detailed treatment of electron-electron correlations.

The s, p, and d orbital radii resulting from our model potential are represented in Fig. 3 and show a strong regularity in the Periodic Table. The S_l values are a measure of the l dependent electronegativity of the core: As S_l gets smaller, the core electronegativity increases. In agreement with this, the orbital radius decreases with the increase of the core charge Z. Down a given column, the behavior is less regular because of the appearance of new core shells. In general, however, the orbital radius increases due to the increase in core size.

III. STRUCTURAL DIAGRAMS

Structural plots based on SB orbital radii have already been applied successfully to $A^N B^{8-N}$ compounds where A and B are nontransition elements.[9,11] The structural coordinates proposed by St. John and Bloch are simple linear combinations of s and p orbital radii because d electrons do not contribute significantly to the formation of covalent bonds in these compounds. These authors define two parameters for each element, namely

$$R_\sigma = S_0 + S_1 , \qquad R_\pi = S_1 - S_0 , \tag{2}$$

and then they define the structural coordinates, which were selected to describe primarily the transition from four fold to six fold coordination, as

$$Y = R_\sigma(A) - R_\sigma(B) , \qquad X = R_\pi(A) + R_\pi(B) . \tag{3}$$

Chelikowsky and Phillips[11] have investigated the physical meaning of Y and X by comparing them to previously used structural coordinates, namely

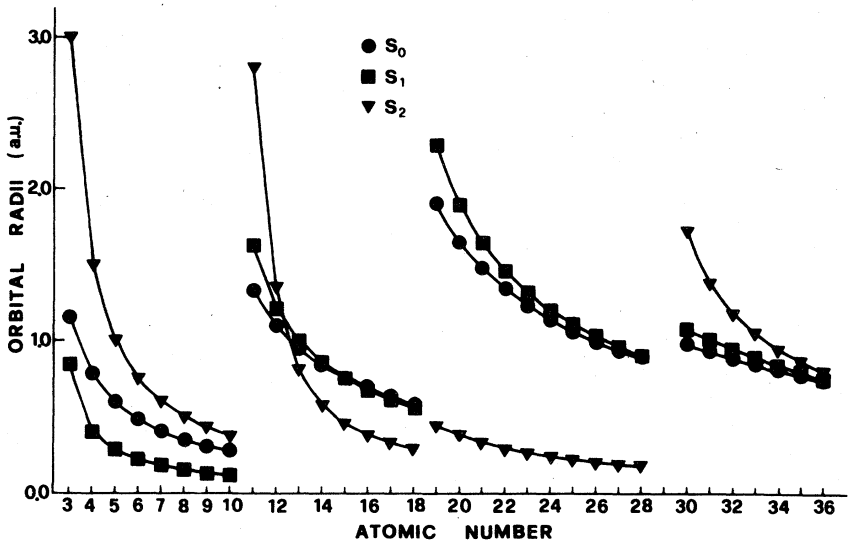

FIG. 3. Regularity of the renormalized orbital radii S_l ($l=0,1,2$) in the Periodic Table.

the Mooser-Pearson[5] coordinates ΔX_{Paul} and $\overline{N}$ and the Phillips-Van Vechten[6] coordinates C and E_h. Although the correlation is not always quantitative, Y and $1/X$ can be qualitatively interpreted as measures of the bond ionicity and of the bond covalency, respectively.

In Fig. 4 we construct the structural plot for $A^N B^{8-N}$ compounds with the St. John-Bloch structural coordinates (3) written in terms of our radii S_0 and S_1. According to our previous discussion (Sec. III), we do not expect that different sets of radii, when combined to give the same coordinates, will give similar plots. The crucial points in the plot of Fig. 4 are Li halides and particularly their X coordinate. As we have already pointed out,[16] in the case of Li-like ions the ratio S_0/S_1 is completely inverted from the SB model to our results [for Li $(S_0^{\text{SB}}/S_1^{\text{SB}})=0.49$ whereas we find $(S_0/S_1)=1.37$], and the R_τ coordinate changes sign (for Li $R_\tau^{\text{SB}}=0.48$, while $R_\tau=-0.31$ in our calculation). According to the St. John-Bloch prescription (2) for R_τ and its interpretation as a measure for s-p hybridization (or tendency to form covalent compounds), large (small) R_τ values (compared to carbon) give weakly (strongly) covalent materials. This scheme correctly predicts Li halides in the intermediate range when the SB radii are used. On the contrary, our S_l values give a negative R_τ for first-row elements. Since the cation is larger, its contribution in the definition of the covalency coordinate is more significant. Thus, a small negative R_τ value for Li (not so much different from carbon) makes Li halides much too covalent.

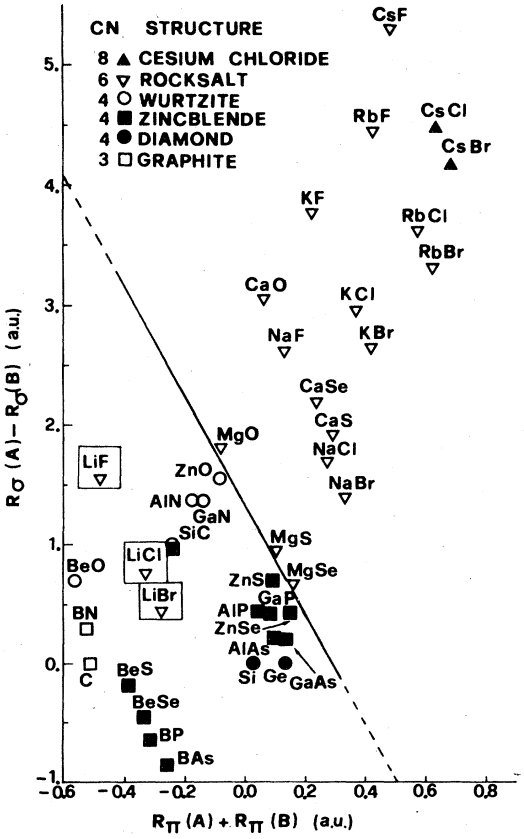

FIG. 4. A structure plot using bond-orbital coordinates derived from renormalized orbital radii. The plot is successful in separating sixfold from fourfold coordination except for the Li salts (boxed).

Because the definition of elemental coordinates (2) is empirical, and because our radii differ from those of SB, the unsatisfactory result shown in Fig. 4 should not be surprising. However, the result of a recent calculation[25] by Zunger and Cohen (ZC) raises a puzzling and rather interesting point. ZC have suggested another set of orbital radii, derived from their local-density pseudopotential calculation for neutral free atoms, and have obtained a successful structural plot with the same definition of R_π and R_σ as used by St. John and Bloch. Their choice of free atoms instead of free ions as elemental constituents of the crystal could represent a good point; however, they never clarify how their eigenvalues compare to HF or experimental energies and how their pseudowave functions compare to actual atomic wave functions, which makes interpreting or reproducing their radii not easy. In an attempt to understand the difference between orbital radii obtained from free atoms and those from free ions, we compare in Fig. 5 the ZC orbital radii[27] S_l^{ZC} to ours for $l=0$ [Fig. 5(a)] and $l=1$ [Fig. 5(b)]. We note that the ZC orbital radii differ from ours since they are defined as the classical turning point of the core pseudopotential that a valence electron with angular momentum l feels in the neutral atom. This difference does not seem to affect the general qualitative trend of the orbital radii. Quantitatively, the ZC s radii are ~18% smaller than ours while their p radii are larger than ours for the first-row atoms and smaller for atoms from the second and third period.

We point out that in Fig. 5(b) we use for the p radius S_1^{ZC} of Li the value 0.9 au, as extrapolated from the ZC p radii of the other first-row atoms and consistent with Fig. 5 of Ref. 27. In their

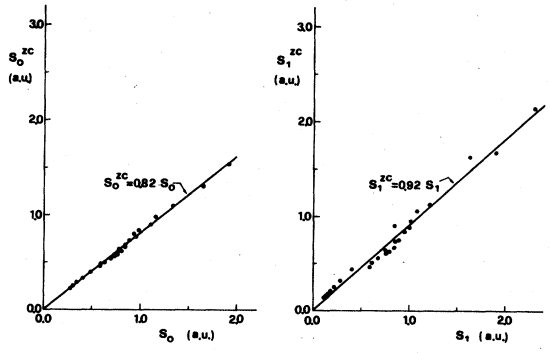

FIG. 5. Comparison between the orbital radii S_l obtained in the present work from an analysis of energy terms and wave functions of free ions and S_l^{ZC} obtained by Zunger and Cohen from free neutral atoms. (a) $l=0$ and (b) $l=1$. All data are in atomic units.

work on structural plots,[26] however, ZC use a value S_1^{ZC} (Li) = 1.465 au which is not reliable. In particular, S_1^{ZC} (Li) $\gg S_0^{ZC}$ (Li) = 0.985 au, which is unphysical because an electron in a $2s$ state sees a core size (S_0) which is larger than that seen by an electron in $2p$ state, since the radial wave function of the former must be orthogonal to that of the $1s$ core electron. Furthermore, we notice that for Li no difference should be expected between ZC radii and ours, because in this case free atom and free ion are the same. In order to resolve this confusion, we have checked further our values of S_1. For Li-like ions (or atoms) a simple analysis of HF $2p$ wave functions immediately gives the following expression of the effective HF potential:

$$V_{\mathrm{HF},l=1}(r) = E_{21}^{\mathrm{HF}} - \frac{\hat{K}\psi_{21}^{\mathrm{HF}}(r)}{\psi_{21}^{\mathrm{HF}}(r)}, \tag{4}$$

where $\hat{K}$ is the kinetic operator and ψ_{21}^{HF} is the one-electron HF wave function. In Table IV we compare HF radii with ours. This test gives S_1^{HF} (Li) = 0.786, in good agreement with our value S_1 (Li) = 0.841, but very different from the ZC value. This result suggests that the ZC value for S_1 (Li) is probably in error.

We stress at this point that the value of the orbital radius of Li is crucial in structural plots. In fact, if one corrects just the p radius of Li in the ZC set and replaces it by 0.9, then the ZC plot strongly resembles the one of Fig. 4. Therefore we consider the success of the ZC structural plot for octet compounds to be somewhat accidental.

In order to solve the structural problem (Fig. 4), we must find new linear combinations R_σ' and R_π' to be used with the new orbital radii. We define

$$R_\sigma' \equiv (S_0 + 3S_1)/4, \tag{5a}$$

where the weighting factor proportional to the

TABLE IV. Values of the turning points S_l calculated with our model pseudopotentials for Li-like ions and of the turning points S_1^{HF} derived from the effective HF potential given in Eq. (4). All turning points are in atomic units.

	S_1^{HF}	S_1
Li	0.786	0.841
Be^+	0.397	0.404
B^{2+}	0.277	0.280
C^{3+}	0.215	0.217
N^{4+}	0.175	0.176
O^{5+}	0.149	0.150
F^{6+}	0.129	0.130
Ne^{7+}	0.115	0.115

state degeneracy is a more appropriate representation of charge transfer, and

$$R_\pi' \equiv (3S_0 - S_1)/4, \tag{5b}$$

which is orthogonal to R_σ' in the same sense as (S_0, S_1) or (R_σ, R_π) are pairs of orthogonal coordinates. The definition (5b) needs further comment. R_π' should be interpreted as the coordinate which measures the difference between the tendency to form sp^3 covalent hybrids (which account for tetrahedral coordination) and the tendency to nonhybridization (p^3 bonding orbitals only). This may explain why the s radius has a larger weighting factor in determining this coordinate.

Structural coordinates are again defined according to Eq. (3) and the resulting plot is shown in Fig. 6. The regularity of the St. John–Bloch plot is completely recovered, and the separation between different domains, which was already excellent, has even improved. A definite straight line separates compounds with fourfold coordination from the sixfold ones which is reminiscent of PVV diagrams.[6] By analogy, this line should define a critical ionicity, and a new scale could accordingly be defined. The separation between wurtzite and zincblende structures is also quite definite, apart from the case of SiC (which indeed crystallizes in a number of different polytypes ranging from zincblende to wurtzite). As noted by Chelikowsky and Phillips, a more elegant separation can be obtained by plotting Y versus X^{-1} (Fig. 7). The quantity X^{-1} plays the role of the covalent energy E_h of Phillips and Van Vechten or the parameter β in Huckel theory.

Our structural plots, Figs. 6 and 7, clearly distinguish among different coordination numbers. Going from the C-BN domain to the CsCl-CsBr region along a line we go from threefold, to fourfold, to sixfold, and eventually to eightfold coordination. Enough crystallographic information exists to separate with a definite straight line fourfold from sixfold coordinated compounds. The same is true within the fourfold coordination domain for the separation between zincblende

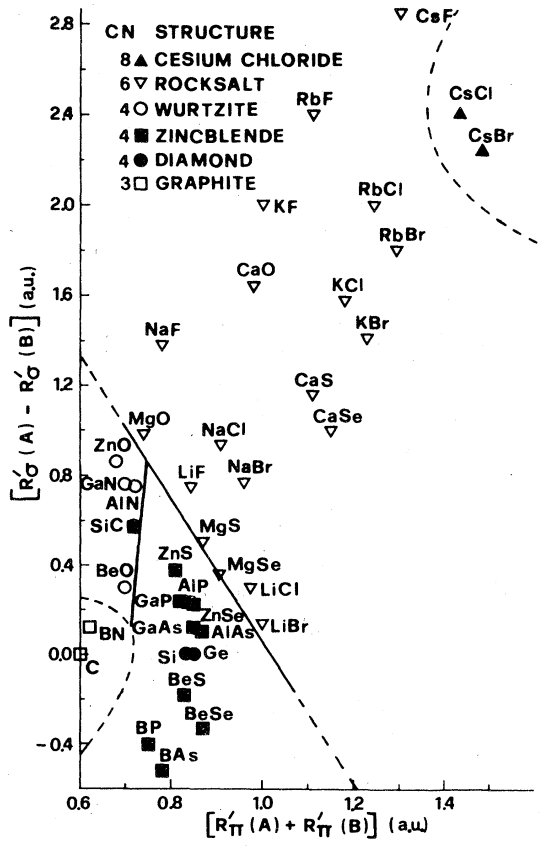

FIG. 6. A structure plot using modified bond-orbital coordinates. The modified coordinates yield a successful structural plot, including Li salts.

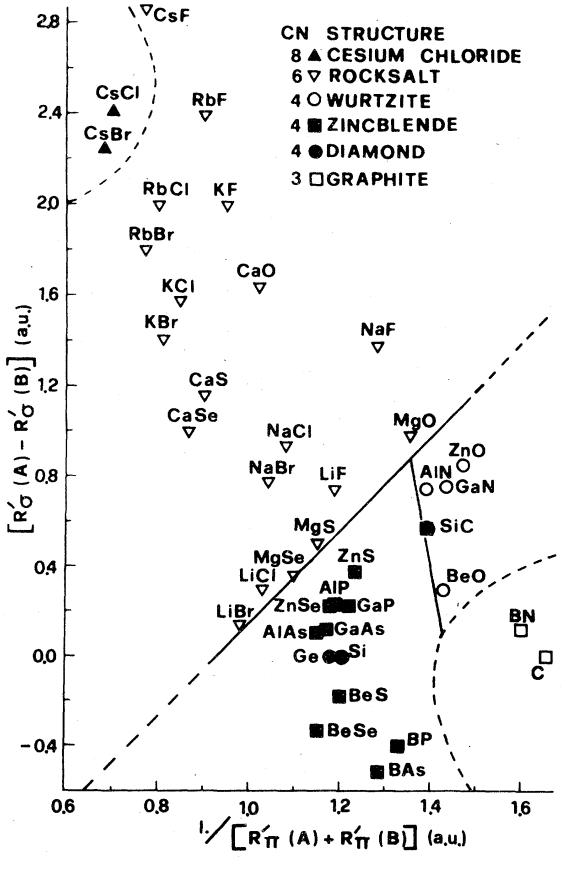

FIG. 7. The plot shown here using the coordinates $((R_\pi')^{-1}, R_0')$ corresponds closely to the Phillips-Van Vechten (E_h, C) plot.

and wurtzite structures. All these separations (represented by solid lines in our plots) are dictated by the high density of data points which are available in these areas of the plots and by the presence of borderline cases such as MgS and MgSe (fourfold-sixfold separation),[28] and SiC (zincblende-wurtzite separation).[29] Threefold-coordinated crystals (BN and graphite) as well as eightfold-coordinated compounds (CsCl and CsBr) are well separated from the compounds with intermediate coordination number, but in these cases, because of the limited number of data points available, definite separation lines cannot be drawn and we have qualitatively indicated the domain boundaries with broken curves.

IV. CONCLUSIONS

We have examined several sets of orbital coordinates defined from hard-core pseudopotentials. Compared to empirically constructed elemental coordinates, the s-p orbital coordinates are manifestly much more successful in describing structural properties and trends of binary intermetallic, semiconducting, and insulating solids formed from nontransition elements. The arbitrariness of the definitions cannot be resolved entirely by comparison with observed crystal structures because of the limited information contained in the latter. However, in all cases, successful results are obtained primarily because of the distinctions made between ionic effects (described by the bond orbital coordinate R_σ) and covalent effects (described by R_π, or more accurately R_π^{-1}). Many other factors, such as the degree of accuracy in fitting to atomic wave functions, or even whether neutral atoms or hydrogenic ions are used to define the coordinates, appear to be of secondary importance, providing that the same definitions and procedures are followed consistently throughout the Periodic Table.

ACKNOWLEDGMENTS

This research was supported in part by the Swiss National Science Foundation. One of the authors (E.B.) wants to acknowledge the Belgian FRFC for financial support.

*Present address: Bell Laboratories, Murray Hill, N.J. 07974.

[1]J. C. Phillips and L. Kleinman, Phys. Rev. 116, 287 (1959).
[2]D. Brust, J. C. Phillips, and F. Bassani, Phys. Rev. Lett. 9, 94 (1962).
[3]C. Herring, Phys. Rev. 57, 1169 (1940).
[4]M. H. Cohen and V. Heine, Phys. Rev. 122, 1821 (1961).
[5]E. Mooser and W. B. Pearson, Acta Crystallogr. 12, 1015 (1959).
[6]J. C. Phillips, Rev. Mod. Phys. 42, 317 (1970); J. A. Van Vechten, Phys. Rev. 182, 891 (1969); 187, 1007 (1969).
[7]G. Simons, Chem. Phys. Lett. 12, 404 (1971).
[8]G. Simons and A. N. Bloch, Phys. Rev. B 7, 2754 (1973).
[9]J. St. John and A. N. Bloch, Phys. Rev. Lett. 33, 1095 (1974).
[10]E. S. Machlin, T. P. Chow, and J. C. Phillips, Phys. Rev. Lett. 38, 1292 (1977).
[11]J. R. Chelikowsky and J. C. Phillips, Phys. Rev. B 17, 2453 (1978).
[12]M. H. Cohen and J. C. Phillips, Phys. Rev. 124, 1818 (1961).
[13]V. Heine and D. Weaire, in *Solid State Physics*, edited by H. Ehrenreich, F. Seitz, and D. Turnbull (Academic, New York, 1970), Vol. 24, p. 249.
[14]K. C. Pandey and J. C. Phillips, Phys. Rev. B 9, 1552 (1974); J. R. Chelikowsky and M. L. Cohen, *ibid.* 14, 556 (1976).
[15]A. Baldereschi and F. Meloni, Proceedings of the Eight EGAS Conference, Oxford, 1976 (unpublished).
[16]W. Andreoni, A. Baldereschi, F. Meloni and J. C. Phillips, Solid State Commun. 24, 245 (1978).
[17]C. Froese-Fischer, Comput. Phys. Comm. 1, 151 (1969); 4, 107 (1972).
[18]A. W. Weiss, Astrophys. J. 138, 1262 (1963); E. Biémont, J. Quant. Spectrosc. Radiat. Transfer 15, 531 (1975); Physica 81C, 158 (1976).
[19]C. Moore, *Atomic Energy Levels* (U.S. GPO, Washington, 1949).
[20]J. P. Desclaux, At. Data Nucl. Data Tables 12, 311 (1973).
[21]R. A. Moore and C. F. Liu, J. Phys. B 12, 1091 (1979).
[22]J. Callaway, Phys. Rev. 106, 868 (1957).
[23]D. W. Norcross, Phys. Rev. A 7, 606 (1973).
[24]J. Migdalek and W. E. Baylis, J. Phys. B 12, 1113 (1979).
[25]J. C. Phillips, Solid State Commun. 22, 549 (1977).
[26]A. Zunger and M. L. Cohen, Phys. Rev. Lett. 41, 53 (1978).
[27]A. Zunger and M. L. Cohen, Phys. Rev. B 18, 5449 (1978); 20, 4082 (1979).
[28]H. Mittendorf, Z. Phys. 183, 113 (1965).
[29]H. Jagodzinski, *Proceedings of the Conference on Silicon Carbide* (Pergamon, New York, 1960), p. 141.